Experimental Study on Predicting Wind-Driven Cross-Ventilation Flow Rates and Discharge Coefficients Based on the Local Dynamic Similarity Model

M. Ohba[1], T. Goto[1], T. Kurabuchi[2], T. Endo[2] and Y. Akamine[3]

[1] Tokyo Polytechnic University, Japan
[2] Tokyo University of Science, Japan
[3] The University of Tokyo, Japan

Abstract

It is known that discharge coefficients vary with wind direction and opening position. The local dynamic similarity model of cross-ventilation can select discharge coefficients on this basis. This paper summarizes previous studies on various inflow opening conditions, and describes new studies on outflow openings and the evaluation of ventilation flow rates in two zones based on coupled simulation of the local dynamic similarity model and a simple network model.

Key words: discharge coefficient, local dynamic similarity model, wind-driven cross-ventilation, ventilation flow rate, inflow opening, outflow opening, network model.

1. Introduction

Natural ventilation is an energy-efficient technology that is adopted to reduce energy consumption for the heating and cooling of buildings. In order to effectively promote the utilization of cross-ventilation, it is important to establish a high-precision model for predicting ventilation flow rate as a basic technique.

When evaluating ventilation flow rates in a wind-driven cross-ventilated building, the traditional orifice model uses fixed discharge coefficients for inflow and outflow openings that are constant regardless of approaching wind direction. However, several studies have shown that discharge coefficients vary with wind direction and opening position (Vickery and Karakatsanis, 1987; Kiyota and Sekine, 1989; Sawachi, 2002). A local dynamic similarity model of cross-ventilation has been developed to explain the variation of discharge coefficient with wind direction, and its validity has been confirmed for inflow openings (Kurabuchi et al., 2004; Ohba et al., 2004; Kurabuchi et al., 2005a).

This paper summarizes previous studies on inflow openings, and describes new studies on outflow openings. It also evaluates the prediction accuracy of ventilation flow rates in two-zone building models based on coupled simulation of the local dynamic similarity model and a simple network model.

2. Local Dynamic Similarity Model for Inflow Opening

Ventilation flow rates (Q) are generally calculated from the orifice equation, and the discharge coefficient (C_d) is assumed to be constant:

$$Q = C_d A \sqrt{\frac{2}{\rho}\left(P_W - P_R\right)} \tag{1}$$

The local dynamic similarity model of cross-ventilation was proposed in order to determine the actual discharge coefficient, which varies with incident angle of approach flow or opening position (Kurabuchi et al., 2004; Ohba et al., 2004; Kurabuchi et al., 2005a).

Figure 1 shows the pressures in the vicinity of the inflow opening. The discharge coefficient (C_d), the inflow angle (β) and the dimensionless room pressure (P_R*) are defined as follows:

$$C_d = \sqrt{\frac{P_n}{\left|P_R - P_W\right|}} \tag{2}$$

$$\beta = \tan^{-1}\sqrt{\frac{P_t}{P_n}} \tag{3}$$

$$P_R* = \frac{P_R - P_W}{P_t} \tag{4}$$

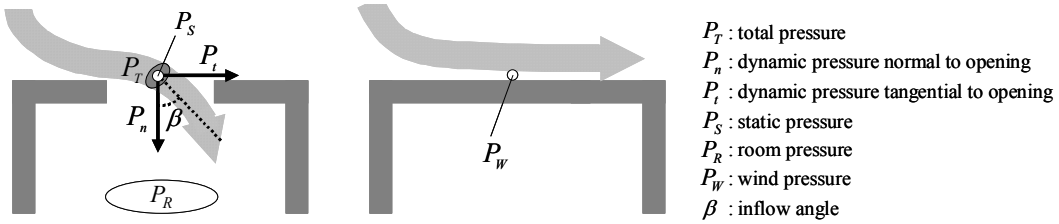

Figure 1. Definition of pressures in the vicinity of inflow opening.

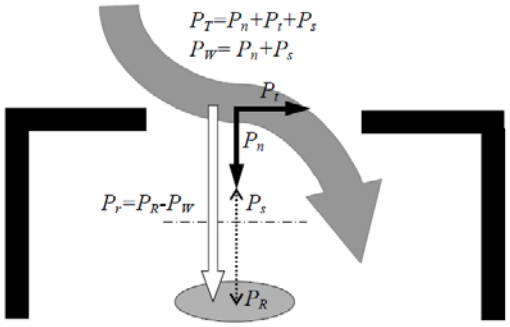

Figure 2. Dynamic similarity in the vicinity of inflow opening (Kurabuchi et al., 2005b).

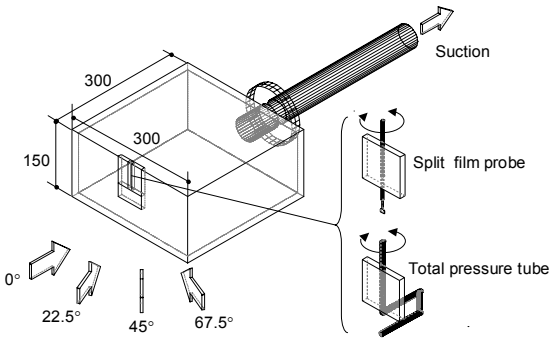

Figure 3. Suction-type ventilation model (Opening size: 60mm × 40mm).

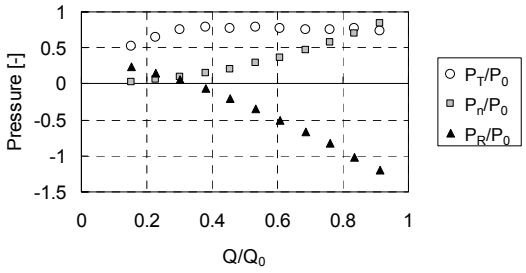

Figure 4. Observed pressures at different flow rates of inflow opening (wind direction: 45°).

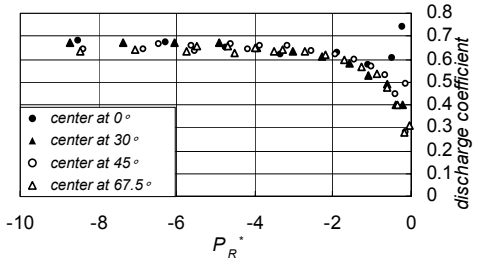

Figure 5. Relationship between P_R and C_d obtained at different wind direction angles.*

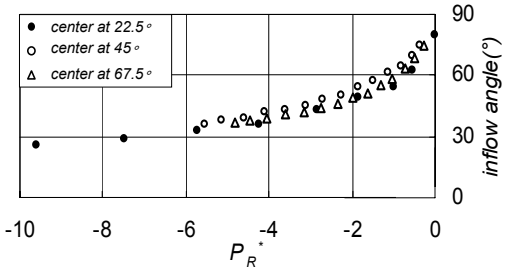

Figure 6. Relationship between P_R and β obtained at different wind direction angles.*

The dimensionless room pressure (P_R*) represents the ratio of cross-ventilation driving pressure $|P_R-P_W|$ and interfering crossflow dynamic pressure P_t (Figure 2). P_R* for an inflow opening is always negative. The proposed model assumes that the discharge coefficient (C_d) and the inflow angle (β) are uniquely determined when P_R* is determined.

Total pressure P_T at an inflow opening is $P_n+P_t+P_S$, as shown in Figure 1. It is assumed that the P_n+P_S is approximately equal to wind pressure P_W, even when ventilation flow is occurring. Thus, P_t can be evaluated as follows:

$$P_t = P_T - P_W \quad (5)$$

Establishment of the local dynamic similarity model may require the following:

a) The opening shape has geometrical similarity;

b) The direction of tangential flow of the approach flow with respect to the opening is constant;

c) The opening is positioned on a wall surface that is sufficiently large with respect to the opening;

d) There is no wall to hinder the diffusion of incoming air flow near the opening on the room side.

To validate the local dynamic similarity model, a wind tunnel experiment was carried out using a suction-type building model that could simulate various ventilation flow rates, as shown in Figure 3. The ventilation flow rates were measured by a thermal flow meter and controlled by a suction fan installed outside the wind tunnel. P_T was measured by a total pressure tube positioned at the centre of the opening, and β was determined by a split film probe. P_R was measured at the ceiling surface of the building model. The approach flow was a boundary layer flow with a power-law index of 0.25, and the reference velocity was kept at 7.0 m/s at the upwind edge of the model.

Figure 4 shows an example of the relation between ventilation flow rate (Q) and three pressure values when the wind direction was 45°. P_T was almost constant regardless of Q, so it could be determined from only the wind direction and the opening position on the wall surface.

The discharge coefficients were measured for various wind directions, and the relation between C_d and P_R* is shown in Figure 5. C_d is almost constant when P_R* is less than -5, and tends to decrease rapidly when P_R* is greater than -2. This relation remains almost constant regardless of the wind direction. Similarly, Figure 6 shows the relation with the inflow angle (β) at the centre of the opening when wind directions are changed. When P_R* increases, the inflow angle β approaches 90°. In this way, it is experimentally demonstrated that the changes of C_d and β can be explained by this local dynamic similarity model.

This was also demonstrated in other experiments under more complicated conditions. One was conducted for the case where another building model was located windward of the ventilation building model, as shown in Figure 7. The relationship between C_d and P_R* was the same as for the isolated building (Figure 8), although the flow pattern around the building was greatly changed by the windward building.

Another experiment was conducted for various opening positions, as shown in Figure 9. The results are shown in Figures 10, 11 and 12 for each opening position height. The relationship between P_R* and C_d at the upper and middle openings was almost consistent with the regression line of the relationship at the central opening (M-2). However, at the lower openings, C_d corresponding to $|P_R*|$ tends to be smaller than that on the regression line, and it is more obvious in the opening position on the windward side. This must be why the crossflow at the lower openings was not parallel to the floor.

3. Local Dynamic Similarity Model for Outflow Opening

Figure 13 shows the pressures in the vicinity of the outflow opening. The discharge coefficient (C_d), the outflow angle (β) and the dimensionless room pressure (P_R*) are defined by the same equations as for the inflow openings (Equations 2 to 4). However, for the outflow opening P_t is the tangential dynamic pressure at the outside end of the opening, and P_S is assumed to be approximately equal to the wind pressure P_W. P_R* for the outflow opening is always positive, unlike that for the inflow opening.

A wind tunnel experiment on an outflow opening was conducted using the blow-type ventilation model shown in Figure 14. This model had two rooms, and air was blown into the windward room by a fan. The wall between the rooms had many

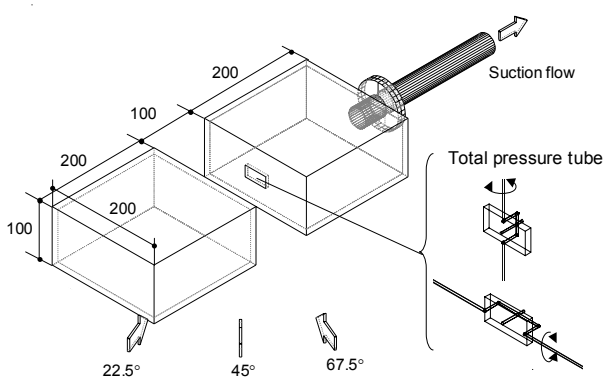

Figure 7. Layout of adjacent building models (Opening size: 40mm × 20mm).

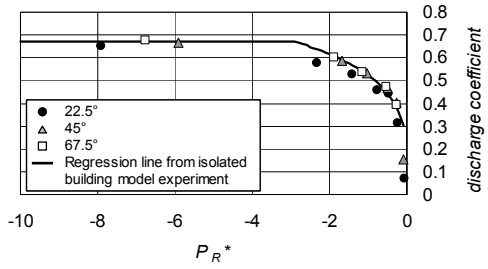

Figure 8. Discharge coefficient curve of leeward ventilation building model.

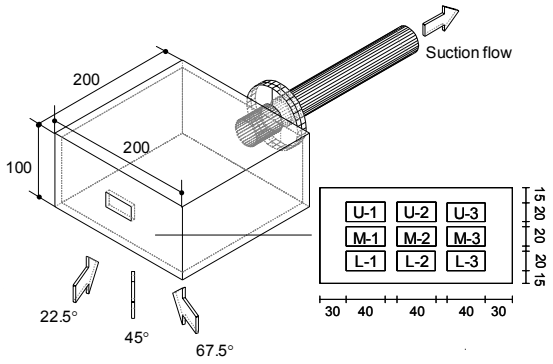

Figure 9. Inflow opening positions.

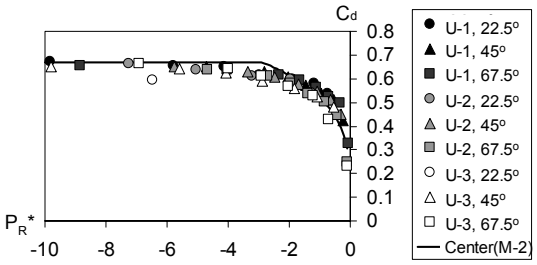

Figure 10. Relationship between P_R and C_d at upper openings.*

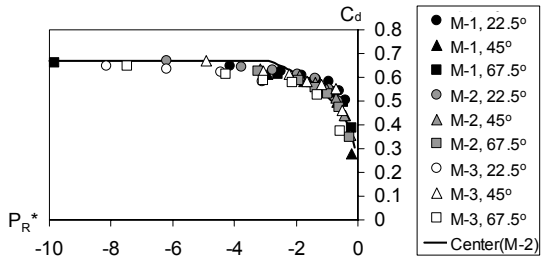

Figure 11. Relationship between P_R and C_d at middle openings.*

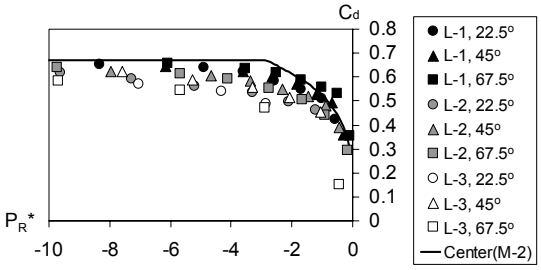

Figure 12. Relationship between P_R and C_d at lower openings.*

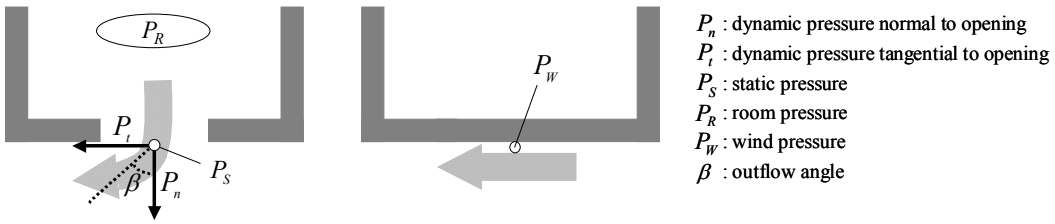

Figure 13. Definition of pressures in the vicinity of outflow opening.

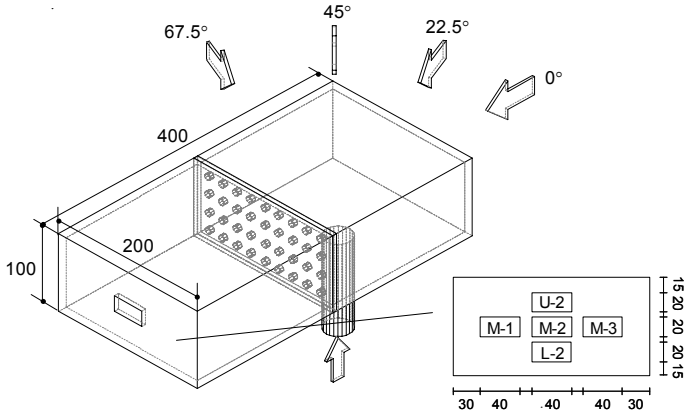

Figure 14. Blow-type ventilation model for outflow openings (Opening size: 40mm × 20mm).

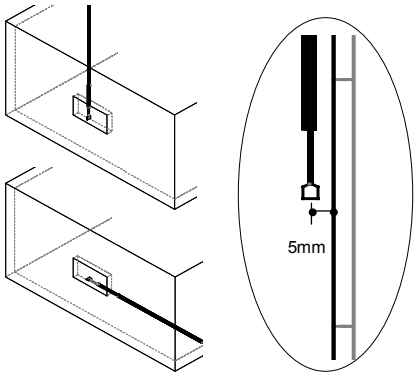

Figure 15. P_t measurement by split film probe.

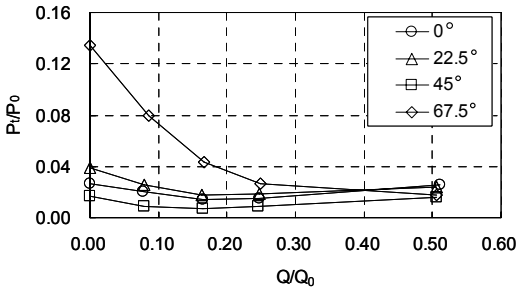

Figure 16. Observed P_t at different flow rates (Measured at 5mm from leeward edge of central opening: M-2).

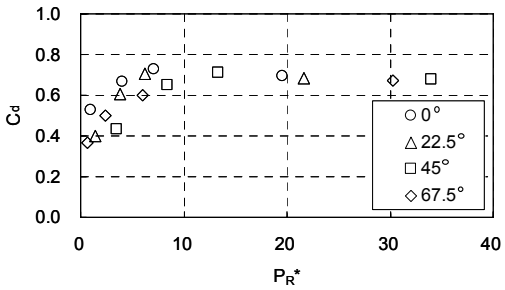

Figure 17. Relations between P_R^* and C_d at central outflow opening (M-2).

small holes of 8 mm diameter, which eliminated the direct influence of blown-out air flow on the internal pressure distribution in the leeward room. The approach flow was a boundary layer flow with a power-law index of 0.25, and the reference velocity was kept at 7.0 m/s at the upwind edge of the model. The incident angle of approach flow was set to 0°, 22.5°, 45°, and 67.5°.

P_t was measured by the split film probe shown in Figure 15. It was found that P_t at 67.5° changed greatly with ventilation flow rate (Figure 16). P_R^* was calculated from P_R, P_W and P_t at each ventilation flow rate, and Figure 17 shows the relationship between C_d and P_R^*. The relationships for all wind directions were very close, and it is inferred that the local similarity model can also be applied to the situation of outflow openings.

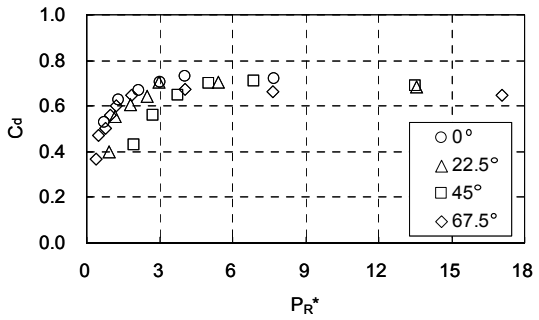

Figure 18. Relationship between P_R and C_d at central outflow opening (P_t=const.).*

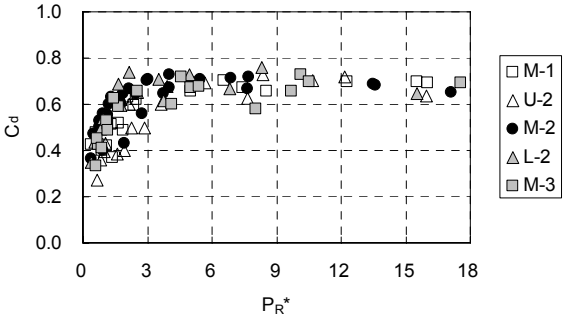

Figure 19. Relationship between P_R and C_d at different outflow opening positions (P_t=const.).*

However, it is impossible to determine P_t at various ventilation flow rates for each situation. Thus, the dynamic pressure tangential to the wall of a sealed building, which is considered to be P_t at Q=0, was measured and applied to calculate P_R* at every ventilation flow rate instead of the actual P_t. As shown in Figure 18, the relationships between C_d and new P_R* at the central opening for all wind directions were still close to each other. Therefore, it is possible to substitute the actual P_t by the P_t measured at Q=0.

Figure 19 shows the relationship between C_d and P_R* at various outflow opening positions. For every opening position, P_t was measured at 5 mm from the wall surface, and used to calculate P_R*. The relationship between P_R* and C_d for all outflow opening positions are similar. It also supports the validity of the local dynamic similarity model for outflow openings.

4. Prediction Accuracy by Local Dynamic Similarity Model for Ventilation Flow Rates in Two Zones

The prediction accuracy for ventilation flow rates based on coupled simulation of the local dynamic similarity model and a simple network model was verified for the two-zone building models shown in Figure 20. The opening was 40 mm wide by 20 mm high. In Case 1, the inflow and outflow openings were located on a straight line. In Case 2, the outflow opening was located at the side-wall of the leeward room. The approach flow was the same as in the previous experiments.

Ventilation flow rates were measured by a tracer gas method for various wind directions. The tracer was generated in the windward room, and its concentration was measured at the leeward edge of the outflow opening by a multi gas monitor

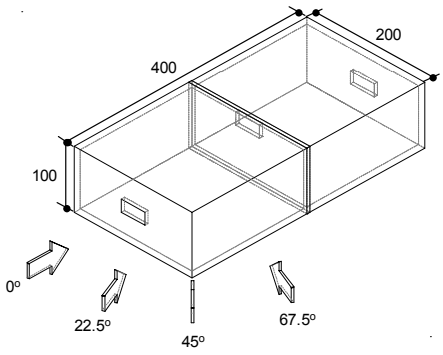

(1) Case 1

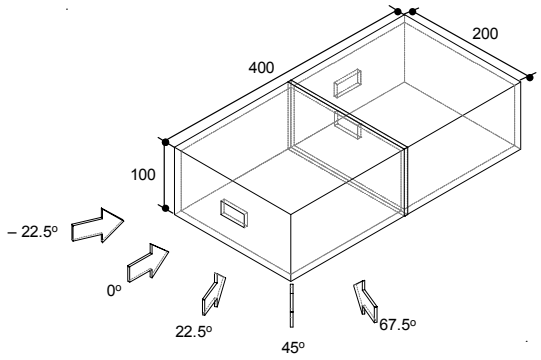

(2) Case 2

Figure 20. Two-zone building models (Opening size: 40mm × 20mm).

(INNOVA A/S) using an extra fine tube that did not disturb the airflow around the model.

In order to apply the local similarity model to the evaluation of ventilation flow rate, the relationships of P_R* and C_d were approximated by the following formula:

$$C_d = C_{dS}\left(\frac{P_R*}{P_{RS}*}\right)^n \qquad \left(|P_R*| \le |P_{RS}*|\right) \qquad (6)$$

$$C_d = C_{dS} \qquad \left(|P_{RS}*| \le |P_R*|\right) \qquad (7)$$

where C_{dS} is the basic discharge coefficient, P_{RS}* is the same as P_R* when C_d is equal to C_{dS}, and n is an empirically fitted parameter. The fitted curves and parameters of ventilation performance for inflow and outflow openings are shown in Figure 21. Figure 22 indicates the procedure for calculation of the ventilation flow rates. P_W and P_t for the building envelope are provided as input data. The ventilation performance of inflow and outflow openings is also provided from Figure 21 as input data. The C_d of the opening on the partition wall is given as a constant value of 0.63 for the present calculation.

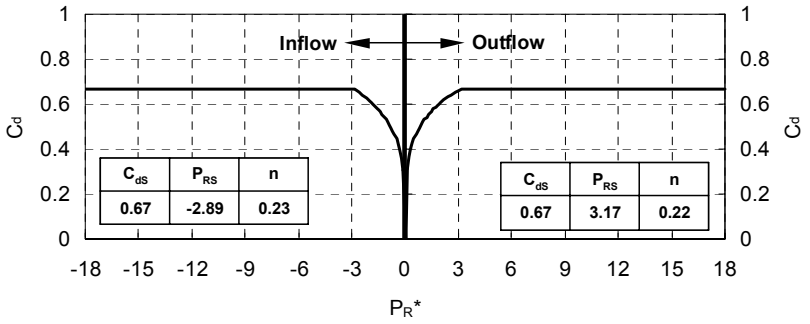

Figure 21. Ventilation performance expressions for inflow and outflow openings.

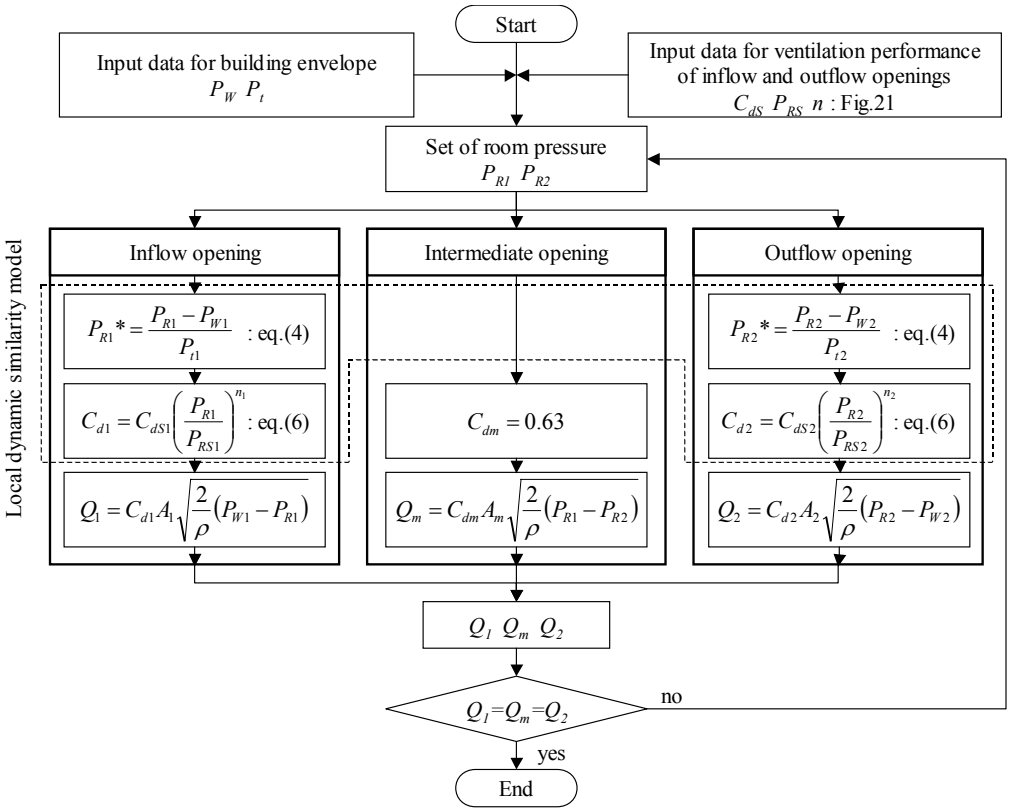

Figure 22. Procedure for calculation of ventilation flow rates based on coupled simulation of local dynamic similarity model and network model for two-zone building models.

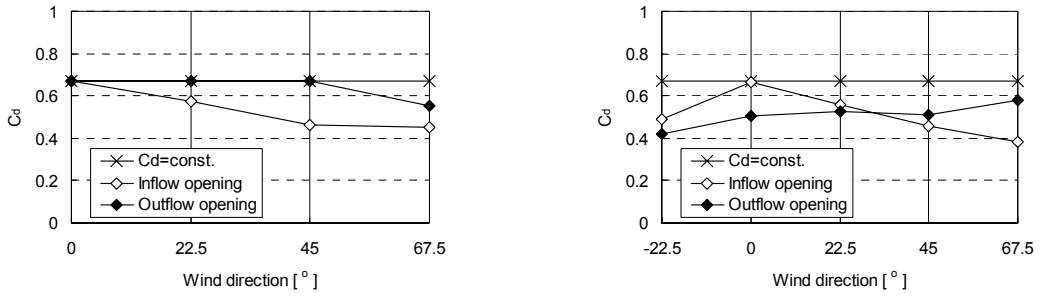

(1) Case 1 *(2) Case 2*

Figure 23. Predicted discharge coefficients at inflow and outflow openings by local dynamic similarity model.

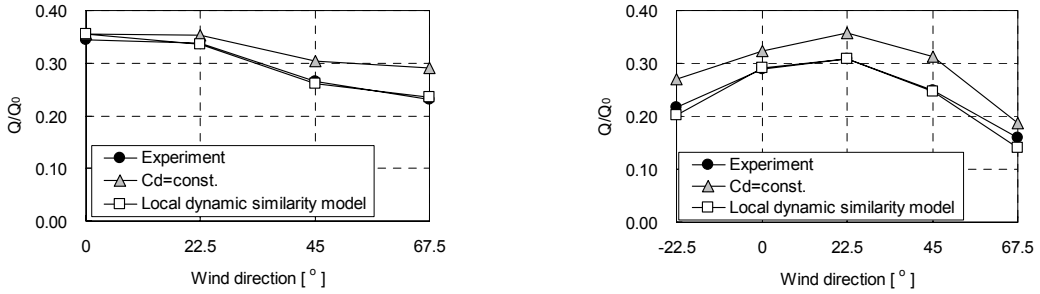

(1) Case 1 *(2) Case 2*

Figure 24. Measured and predicted ventilation flow rates.

The internal pressures of the two rooms are initially assumed. For the inflow opening, P_{R1}* and C_{d1} are calculated using Equations (4) and (6). The ventilation flow rate is determined using C_{d1} and the pressure difference between P_{W1} and P_{R1}. For the outflow opening, the same calculation procedure is performed. The iteration continues until $Q_1=Q_m=Q_2$.

Figure 23 indicates the discharge coefficients at inflow and outflow openings by the local dynamic similarity model. In Case 1, the local dynamic similarity model finally selects discharge coefficients of 0.45 for the inflow opening and 0.55 for the outflow opening, when the wind direction is 67.5°. However, the orifice model uses a C_d of 0.67 for both inflow and outflow openings, regardless of wind direction. In Case 2, the predicted C_d greatly varies in the range of -22.5° to 67.5°.

Figure 24 compares the evaluated ventilation flow rates with the measurements as well as those by the conventional orifice model (C_d=const.). The prediction accuracy for wind direction 67.5° of Case 1 is improved by 24% by the local dynamic similarity model. In Case 2, the local dynamic similarity model indicates better predictions for all wind directions than the conventional orifice model. In this case, the orifice model cannot predict the ventilation flow rate accurately, because the interfering crossflow dynamic pressure P_t is too high at either inflow opening or outflow opening.

5. Simplified Method for Estimating P_t on a Building Wall Surface

In order to utilize the local dynamic similarity model, the data of tangential dynamic pressure P_t is required as a parameter, as shown in Equation (4). As shown above, total pressure P_T was measured for the inflow openings, and "P_T-P_W" was determined instead of P_t. P_t measurement with a hot-wire anemometer, as applied for outflow openings, is also available for inflow openings (Kurabuchi et al., 2004; Ohba et al., 2004). Thus, no openings are necessary with a building model when the

ventilation performance is investigated at the design stage. However, it is still hard to determine the P_t distribution on a building wall surface using a hot-wire anemometer.

In order to solve this problem, a new method using Irwin's surface wind sensor (Irwin, 1981) has been proposed. The details of this method were previously reported (Kurabuchi et al., 2005a). With this method, the P_t distribution on a building wall surface can be obtained without much time and work.

6. Conclusions

The present study yielded the following conclusions:

- For inflow openings, it was confirmed that the discharge coefficient can be predicted by a single parameter of dimensionless room pressure P_R* regardless of wind direction, opening position and building location, unless the crossflow direction is greatly changed. The total pressure at the inflow opening is constant regardless of the ventilation flow rate.
- For outflow openings, the relationships of discharge coefficient C_d to P_R* were similar even when the wind directions and opening positions were varied. It is possible to estimate the discharge coefficient by a single parameter of dimensionless room pressure P_R*. The tangential dynamic pressure P_t at the outflow openings was not constant, but it could be substituted by the P_t measured close to the wall of a sealed building.
- The local dynamic similarity model coupled with a simple network model indicated better prediction accuracy of ventilation flow rates in two rooms than the conventional orifice model.
- P_t distribution on a building wall surface can be obtained easily by using Irwin's wind surface sensor.

Acknowledgement

This study was partially funded by the Ministry of Education, Culture, Sports, Science and Technology, Japan, through the 21st Century Center of Excellence Program of Tokyo Polytechnic University.

Nomenclature

A	opening area
C_d	discharge coefficient
C_{dS}	basic discharge coefficient
n	power exponent
Q	ventilation flow rate
Q_0	reference ventilation flow rate ($=AU_0$)
P_n	dynamic pressure normal to opening
P_0	dynamic pressure of reference velocity ($=\rho U_0^2/2$)
P_R	room pressure
P_R*	dimensionless room pressure
P_{RS}*	dimensionless room pressure in case of $C_d = C_{dS}$
P_S	static pressure
P_t	dynamic pressure tangential to opening
P_T	total pressure
P_W	wind pressure
U_0	reference wind velocity at rooftop
β	inflow angle or outflow angle
ρ	density

References

Irwin HPAH: (1981) "A simple omnidirectional sensor for wind-tunnel studies of pedestrian-level winds", *Journal of Wind Engineering and Industrial Aerodynamics*, 7, pp219-239.

Kiyota N and Sekine T: (1989) "Experiment study on pressure loss at the opening of wall surface (Part2)", *Journal of Architecture and Planning, Architectural Institute of Japan*, (398), pp47-57.

Kurabuchi T, Ohba M, Endo T, Akamine Y and Nakayama F: (2004) "Local dynamic similarity of cross-ventilation, Part 1 Theoretical framework". *International Journal of Ventilation*, **2**, (4), pp371-382.

Kurabuchi T, Ohba M, Goto T, Akamine Y, Endo T and Kamata M: (2005a) "Local dynamic similarity concept as applied to the evaluation of discharge coefficients of cross ventilated buildings, Part 1 Basic idea and underlying wind tunnel tests; Part 2 Applicability of local dynamic similarity model; Part 3 Simplified method for estimating dynamic pressure tangential to openings of cross-ventilated buildings", *International Journal of Ventilation*, **4**, (3), pp285-300.

Kurabuchi T, Akamine Y, Ohba M, Endo T, Goto T and Kamata M: (2005b) "A study on the effects of

porosity on discharge coefficient in cross-ventilated buildings based on wind tunnel experiment", *Proceedings of the 2nd International Workshop on Natural Ventilation*.

Ohba M, Kurabuchi T, Endo T, Akamine Y, Kamata M and Kurahashi A: (2004) "Local dynamic similarity of cross-ventilation, Part 2 Application of local similarity model", *International Journal of Ventilation*, **2**, (4), pp383-393.

Sawachi T: (2002) "Detailed observation of cross ventilation and airflow through large openings by full scale building model in wind tunnel". *Proceedings of the 8th International Conference on Air Distribution in Rooms (ROOMVENT 2002)*, pp565-568.

Vickery BJ and Karakatsanis C: (1987) "External wind pressure distribution and induced internal ventilation flow in low-rise industrial and domestic structures", *ASHRAE Transactions*, **93**, Part 2, pp2198-2213.